BMC Cardiovascular Disorders

RESEARCH

Open Access

Isoliquiritigenin attenuates myocardial ischemia reperfusion through autophagy activation mediated by AMPK/mTOR/ULK1 signaling

Liying Shen[1], Yingwei Zhu[1], Zhenfeng Chen[1], Feng Shen[1], Weiwei Yu[1] and Li Zhang[1*]

Abstract

Background Ischemia reperfusion (IR) causes impaired myocardial function, and autophagy activation ameliorates myocardial IR injury. Isoliquiritigenin (ISO) has been found to protect myocardial tissues via AMPK, with exerting anti-tumor property through autophagy activation. This study aims to investigate ISO capacity to attenuate myocardial IR through autophagy activation mediated by AMPK/mTOR/ULK1 signaling.

Methods ISO effects were explored by SD rats and H9c2 cells. IR rats and IR-induced H9c2 cell models were established by ligating left anterior descending (LAD) coronary artery and hypoxia/re-oxygenation, respectively, followed by low, medium and high dosages of ISO intervention (Rats: 10, 20, and 40 mg/kg; H9c2 cells: 1, 10, and 100 μmol/L). Myocardial tissue injury in rats was assessed by myocardial function-related index, HE staining, Masson trichrome staining, TTC staining, and ELISA. Autophagy of H9c2 cells was detected by transmission electron microscopy (TEM) and immunofluorescence. Autophagy-related and AMPK/mTOR/ULK1 pathway-related protein expressions were detected with western blot.

Results ISO treatment caused myocardial function improvement, and inhibition of myocardial inflammatory infiltration, fibrosis, infarct area, oxidative stress, CK-MB, cTnI, and cTnT expression in IR rats. In IR-modeled H9c2 cells, ISO treatment lowered apoptosis rate and activated autophagy and LC3 fluorescence expression. In vivo and in vitro, ISO intervention exhibited enhanced Beclin1, LC3II/LC3I, and p-AMPK/AMPK levels, whereas inhibited P62, p-mTOR/mTOR and p-ULK1(S757)/ULK1 protein expression, activating autophagy and protecting myocardial tissues from IR injury.

Conclusion ISO treatment may induce autophagy by regulating AMPK/mTOR/ULK1 signaling, thereby improving myocardial IR injury, as a potential candidate for treatment of myocardial IR injury.

Keywords Isoliquiritigenin, Autophagy, Ischemia reperfusion injury, AMPK/mTOR/ULK1

Introduction

Acute myocardial infarction and ischemic heart disease are cardiovascular diseases that have affected human health worldwide with extremely high morbidity and mortality [1]. Although myocardial reperfusion therapy is an effective therapeutic measure to diminish myocardial infarction area and restore coronary blood supply, however, this therapeutic process induces cardiomyocyte

*Correspondence:
Li Zhang
zhanglinbu2010@163.com
[1] Department of Cardiology, Huzhou Central Hospital, No. 1558, Sanhuan North Road, Wuxing District, Huzhou 313000, Zhejiang, China

death and contributes to myocardial functional impairment, known as myocardial ischemia reperfusion (IR) injury [2, 3]. The pathogenesis of IR that has been demonstrated to date is complicated, involving mitochondrial dysfunction, oxidative stress, inflammatory response, and calcium overload [4, 5]. Identifying effective therapeutic medications or treatments to attenuate myocardial IR injury has become a pressing task that requires immediate attention and action.

Isoliquiritigenin (ISO) is a naturally derived flavonoid compound from *Glycyrrhiza uralensis,* which possesses a wide range of pharmacological effects and biological activities, that includes anti-inflammatory, antioxidant, anti-atherosclerotic, and anti-tumor effects [6, 7]. ISO has been proven to have protective potential against cerebral and myocardial IR injury [8, 9]. It has been demonstrated that ISO attenuated myocardial IR injury in rats through activation of JAK2/STAT3 signaling pathway [9]. More recently, ISO treatment was identified to have cardio-protective effects by attenuation of oxidative stress and inflammatory responses through modulation of Nrf2/HO-1 pathway in mice with acute myocardial infarction [10]. In addition, ISO treatment was able to modulate apoptosis and autophagy activity through alteration of multiple targets, and activate autophagy, thus inhibiting tumorigenesis [11, 12].

Autophagy holds a key role in myocardial IR injury [13]. Autophagy is unactivated after occurrence of IR, with an decrease in autophagic vesicles [3]. Loos et al. performed ischemia simulation using H9c2 cells, but found mild ischemia resulted in increased levels of myocardial autophagy [14]. In fact, restoration of damaged cardiomyocyte autophagy led to myocardial IR injury attenuation [13]. Shexiang Baoxin Pill has been proved to decrease IR injury by activating autophagy through regulation of ceRNA-Map3k8 pathway [15]. In addition, APMK-mTOR-ULK1 signaling pathway was identified to mediate autophagy to protect cerebral IR rats, which may be a new target for cerebral IR injury treatment by regulating autophagy [16].

Under myocardial IR-induced oxidative stress, mitochondrial oxidative phosphorylation levels reduces and then ATP production decreases, which trigger AMPK, thereby up-regulating mTOR-ULK1 signaling, and subsequently autophagy gets activated [3]. ISO treatment has been shown to improve contractile dysfunction in hypoxic cardiomyocytes by AMPK signaling, protecting heart from ischemic injury [17]. Meanwhile, in vivo and in vitro, it has been observed that ISO treatment may act to induce apoptosis through activation of autophagy in hepatocellular carcinoma cells through PI3K/Akt/mTOR pathway [12]. Moreover, a major component of Ginseng has been investigated to alleviate myocardial fibrosis in mice through AMPK/mTOR/ULK1 signaling-mediated autophagy activation [18]. Currently, whether ISO treatment protects heart from IR injury through AMPK/mTOR/ULK1 signaling pathway still deserves further investigation and exploration.

Hence, the present study was conducted to investigate mechanism of ISO treatment in its ability to mitigate myocardial IR injury, for further development of ISO as an effective therapeutic strategy to protect cardiac function from IR injury.

Materials and methods

Ethic statement

The Animal Experimentation Ethics Committee of Zhejiang Eyong Pharmaceutical Research and Development Centre approved the ethical conduct of animal experiments (SYXK(Zhe) 2023–0027).

Animals

30 male SD rats weighing 200–230 g (6–8 weeks) were obtained from Shanghai Jihui Laboratory Animal Care Co, Ltd. (License number: SCXK (Hu) 2022–0009), and subsequently accommodated in at Zhejiang Eyong Pharmaceutical R&D Co., Ltd (license number: SYXK (Zhe) 2023–0027). The rearing temperature for these rats was maintained at 22–25 °C, with a relative humidity of 55% and exposed to a 12 h light/dark cycle. All rats had access to both food and water at all times. Prior to administration, acclimatization of rats for a week was conducted.

Experiment design

The rats were randomly assigned to five groups with random number table approach ($n=6$): Control (Con), IR, IR + ISO Low-dose-treated (ISO-10) (10 mg/kg), IR + ISO Middle-dose-treated (ISO-20) (20 mg/kg), and IR + ISO High-dose-treated (ISO-40) (40 mg/kg) groups on the basis of previous research [19]. All rats were given daily gavage administration for 30 consecutive days and then the establishment of IR model was conducted.

IR rat modeling

The procedure of IR modeling method in our study was carried out by referring to the method previously described [20]. After anesthetizing rats with 1.5% isoflurane, the left anterior descending (LAD) coronary artery was blocked by ligation for 30 min, and then the sutures were loosened for 2 h to establish IR rat model. We observed the presence of significant pallor in the left ventricle, in conjunction with ischemia achieved by ST-segment elevation on electrocardiographic monitoring. In Control group, the same operation was performed on rats without LAD coronary artery ligation. All rats were

successfully modeled to complete subsequent experiments, with no death occurred.

Cardiac function measurement

Cardiac function was assayed 24 h after successful IR rat modeling. After rats in each group were anesthetized with 1.5% isoflurane by inhalation, their cardiac function was evaluated by a *VEVO 770* High-Resolution Imaging System (Visual Sonics, Canada). The left ventricular end-systolic diameter (LVESD), left ventricular end-diastolic diameter (LVEDD), ejection fraction (EF), fractional shortening (FS), left ventricular peak systolic pressure (LVSP), and left ventricular end diastolic pressure (LVEDP) measurements in all rats were recorded using two-dimensional, *M-Mode* echocardiography.

Sample collection

After detecting cardiac function of all rats and confirming that they were completely under anesthesia, we cut their abdomens open, and approximately collected 3 mL blood from the main abdominal vein. Subsequently, with centrifugation at 3500 rpm for 15 min, the supernatant was collected and utilized to determine creatine kinase-MB (CK-MB), cardiac troponin-I (cTnI), and cardiac troponin-T (cTnT) expression with ELISA kits afterwards. The rats were euthanized following blood sampling by inhalation of compressed CO_2 (30% V/min) in cylinders. And then the hearts were rapidly isolated, with apical 1/3 to 2/3 of hearts prepared as paraffin sections for HE staining to observe inflammatory cell infiltration. The apical 1/3 of hearts was frozen at -80 °C for subsequent Western blot assay.

HE staining

The apical 1/3 to 2/3 of rat hearts was fixed with 4% paraformaldehyde, embedded in paraffin, sectioned, and stained with hematoxylin (H3136, sigma) and eosin (E4009, sigma) to assess histopathological changes in border areas of rat cardiac tissues. The assessment was performed by individuals not involved in experimental process.

Masson trichrome staining

Following deparaffinization of paraffin sections, Weigert iron hematoxylin staining for 10 min and acidic compound red-Lichun red solution (71,019,360, 71,033,761, Sinopharm Chemical Reagent Co.,Ltd) staining for 5–10 min were sequentially performed. Subsequently, phosphomolybdic acid solution (XW514297441, Beijing Wokai Biotech Co.) staining for 3–5 min and aniline blue solution (71,003,644, Sinopharm Chemical Reagent Co.,Ltd) staining for 1–5 min were done. Then, the dehydration, placing in xylene for soaking, sealing and observation were made. Under the microscope, the cell nucleus exhibited blue-black, with collagen fibers and mucus blue, and myofibrils, fibrils and erythrocytes orange-red.

TTC staining

The perfusion was performed for collection of heart weighed and sectioned in 6 segments (1–2 mm thick). The samples were stained using 1% TTC solution (F603BA0025, Shenggong Biotechnology Engineering Co.) at 37 °C for 15 min. Photography was taken following 4% paraformaldehyde fixation for 30 min. The areas of non-infarcted area (red) and infarcted area (white) were analyzed and calculated. Infarcted areas of cardiac tissues (%) = infarcted areas of the heart/total areas of the heart × 100%

ELISA

The supernatant was taken and we followed instruction steps of the rat CK-MB ELISA kit (CB10461-Ra, COIBO), rat cTn-I ELISA kit (RX302234R, RuiXin), rat cTnT ELISA kit (RX301216R, RuiXin), Total-superoxide dismutase (T-SOD) kit (A001-1, NanJing JianCheng Bioengineering Institute), malondialdehyde (MDA) kit (A003-1, NanJing JianCheng Bioengineering Institute), and glutathione (GSH) kit (A006-2–1, NanJing JianCheng Bioengineering Institute) to estimate contents of CK-MB, cTnI, cTnT, T-SOD, MDA, and GSH levels. The absorbance values were calculated at 450 nm.

Cell culture, treatment and grouping

Rat cardiomyocytes H9c2 cells (iCell-r012, iCell Company) were cultured with reference to method previously described [21]. The logarithmically grown H9c2 cells were randomly classified into five groups: Control (Con), IR model (IR), IR + 1 μmol/L ISO (IR + ISO-1), IR + 10 μmol/L ISO (IR + ISO-10), and IR + 100 μmol/L ISO (IR + ISO-100) groups on the basis of previous research [11]. Cells in Control group were cultured in normal conditions (21% O_2, 5% CO_2, 37 °C) without any treatment. Following 8 h incubation in serum-free medium containing corresponding concentration of ISO, H9c2 cells of IR + ISO-1, IR + ISO-10, and IR + ISO-100 groups underwent modeling processes.

We followed previously described protocols to establish myocardial IR model in H9c2 cells [21]. To simulate ischemia, after rinsing cells three times with PBS, they were cultured in glucose-free DMEM at 37 ℃ under light protection and hypoxic conditions (94% N_2, 5% CO_2, and 1% O_2) for 4 h. Subsequently, reperfusion was simulated by replacing the glucose-free DMEM with complete DMEM containing 4.5 mg/mL glucose). The cells were incubated in a 37 °C incubator with 95% air and 5% CO_2.

Cell samples were obtained after reperfusion period of 24 h.

Cell counting kit-8 (CCK-8)

H9c2 cells were seeded into 96-well plates and cultured for 48 h, followed by adding CCK8 solution (10 μL) to each well and incubating at 37 °C for 4 h. The absorbance was calculated by a microplate spectrophotometer at 450 nm.

Flow cytometry (FC)

To determine the apoptosis rate of H9c2 cells, FC assay was conducted in accordance with instructions of Apoptosis Kit (556,547, BD). The collection of H9c2 cells was done at a concentration of 1×10^6 cells/mL, and addition of 500 μL of binding buffer, centrifugation, and subsequent addition 100 μL of binding buffer was performed. The reaction was carried out at room temperature, avoiding light for 15 min, following addition of 5 μL Annexin V-FITC and 10 μL PI. The final 400 μL of binding buffer was added, and detection of apoptosis rate was made by FC assay within 1 h.

Transmission *electron* microscopy (TEM)

The collected cells were fixed in 2.5% glutaraldehyde solution for 4 h, rinsed, and then fixed in 1% osmium acid solution for 1–2 h. Following dehydration treatment with gradient concentrations of ethanol solution, H9c2 cells were embedded, sectioned (50–70 nm thickness), and subsequently completed with uranyl acetate and lead citrate staining. Samples were placed under transmission electron microscope to view ultra-structural changes.

Immunofluorescence

The H9c2 cells were fixed with 4% paraformaldehyde, permeabilized with 0.5% Triton X-100, and blocked with serum. Cells were incubated overnight at 4 °C with primary antibody (AF5402, Affinity), and then Goat-Anti-Rabbit lgG (Alexa FLIOR 488) (ab150077, Abcam) was added with incubation at room temperature for 1 h. After counter-staining of cell nuclei with DAPI, observation was performed with a fluorescence microscope (Ts2-FC, Nikon).

Western blot

After protein extraction of rat myocardial tissues in infarct and non-infarct areas and H9c2 cells, quantification was accomplished with a BCA kit (pc0020, Beyotime). With separation by 10% SDS-PAGE gel electrophoresis, protein transferring to PVDF membranes (10,600,023, GE Healthcare Life) was completed. Primary antibodies (Table 1) were incubated at 4 °C overnight, followed by block with 5% milk. Subsequent secondary antibodies (Table 1) incubation was performed. Protein bands were detected by chemiluminescence (610,020-9Q, Clinx) and band analysis was done by ImageJ.

Table 1 Antibody information

Antibody	Company	Article Number
Anti-Beclin 1 Antibody	Abcam	ab210498
Anti-SQSTM1/p62 Antibody	Abcam	ab91526
Anti-LC3 Antibody	Abcam	ab192890
Phospho-AMPK alpha (Thr172) Antibody	Affinity	AF3423
Anti-AMPK alpha Antibody	Affinity	DF6361
Anti-mTOR Antibody	Abcam	ab2732
Anti-Phospho-mTOR Antibody	Abcam	ab109268
Anti-ULK1Antibody	Abcam	ab177472
Phospho-ULK1 (Ser757) Antibody	Affinity	AF4387
Phospho-ULK1 (Ser555) Antibody	Affinity	AF7148
Anti-rabbit IgG, HRP-linked Antibody	CST	7074
GAPDH Antibody	Proteintech	10,494–1-AP

Statistical analysis

SPSS 20.0 statistical software was used to analyze these data. The one-way-ANOVA was employed when measurement information between multiple groups met the normal distribution and Chi-square test, and further two-by-two comparisons between groups were performed by Turkey test. The analysis of data that did not conform to normal distribution was done by Kruskal–Wallis H-test. All data were expressed as mean ± standard deviation. The level of significance was $\alpha = 0.05$, with $P < 0.05$ considered statistically significant.

Results

ISO treatment attenuated myocardial injury and oxidative stress in IR rats

Flowchart of our experiments in rats was constructed as presented in Fig. 1A. Assessment of cardiac function was accomplished with echocardiography in all rats, including LVESD, LVEDD, EF, FS, LVSP, and LVEDP levels (Fig. 1B). On completion of IR modelling, rats had higher LVEDD values and lower EF and FS values ($P < 0.01$). EF and FS values of IR rats were significantly elevated with three different doses of ISO treatment ($P < 0.01$). Meanwhile, LVEDD values of IR rats in ISO-20 and ISO-40 groups was lower ($P < 0.05$ or $P < 0.01$). The IR rats demonstrated higher LVEDP values, whereas lower LVSP values than those of control rats ($P < 0.01$). There were reduced LVEDP levels occurred following ISO treatment at 10, 20, and 40 mg/kg ($P < 0.05$ or $P < 0.01$), with enhanced LVSP levels ($P < 0.05$ or $P < 0.01$). As presented in Fig. 1C, in comparison with normal myocardial tissue

structure and well-arranged cardiomyocytes of Control group rats, IR rats suffered severe damage to cardiac tissues, with massive inflammatory cell infiltration, extensive tissue fibrosis, enlarged cell gaps, and disorganized cardiomyocyte arrangement. The ISO treatment contributed to varying degrees of improvement on cardiac tissue damage, alleviated cell gap enlargement, and decreased in inflammatory cell infiltration and tissue fibrosis (Fig. 1C). Observation of fibrosis in rat heart tissues was made by Masson staining (Fig. 1D). The heart tissue structure of control rats exhibited basically normal, which basically consisted of a large amount of red-stained normal heart tissue. IR rats demonstrated severe cardiac tissue damage, with massive deposition of blue-stained collagen fibers. Following ISO treatment, IR rat cardiac tissue damage was attenuated, with lower blue-stained collagen fiber deposition. Furthermore, the CVF of IR rats exhibited an increase than control rats ($P<0.01$). In IR + ISO-10, IR + ISO-20, and IR + ISO-40 groups, there was lowered CVF values occurred than in IR groups ($P<0.05$ or $P<0.01$). In Fig. 1E, the TTC staining was utilized to determine the infarcted area of rat heart tissues. The IR rats exhibited increased infarction rate than that of control rats ($P<0.01$). Following ISO intervention, infarction rate of IR rat cardiac tissues reduced than in IR group ($P<0.01$).

After ELISA detection of myocardial infarction-associated factors in all rats, we found that plasma levels of CK-MB, cTnI, and cTnT in IR group revealed elevated values relative to those of Control group (Fig. 1F-H, $P<0.01$). Moreover, CK-MB, cTnI, and cTnT levels of ISO-10, ISO-20, and ISO-40 groups were reduced compared with IR group ($P<0.01$). The detection of MDA, SOD, and GSH levels in rat cardiac tissues was carried out (F ig. 1I-K). The IR rats demonstrated higher MDA levels ($P<0.01$), whereas lower SOD and GSH levels than those of control rats ($P<0.05$ or $P<0.01$). The IR + ISO-10, IR + ISO-20, and IR + ISO-40 groups led to reduced MDA levels ($P<0.01$), with increased SOD and GSH levels than IR rats ($P<0.05$ or $P<0.01$).

ISO treatment induced autophagy by AMPK/mTOR/ULK1 pathway in IR rats

In Fig. 2A-B, measurement of Beclin1, P62, and LC3II/LC3I protein expression in non-infarcted and infarcted areas of rat myocardial tissues was constructed by western blot assay. In rat myocardial tissue non-infarcted areas displayed in Fig. 2A, IR group indicated diminished Beclin1 and LC3II/LC3I levels, whereas enhanced P62 protein expression ($P<0.01$). In IR + ISO-10 group, there was higher Beclin1 protein expression and lower P62 expression than IR group rats ($P<0.05$ or $P<0.01$). We found that IR rats in IR + ISO-20 and IR + ISO-40 groups led to increased Beclin1 and LC3II/LC3I levels ($P<0.05$ or $P<0.01$), whereas reduced P62 protein expression in myocardial tissues ($P<0.01$). In Fig. 2B, there were lowered Beclin1 and LC3II/LC3I protein levels ($P<0.01$), whereas increased P62 levels in rat myocardial tissue infarction areas ($P<0.01$). The ISO treatment at 10 mg/kg led to higher LC3II/LC3I protein levels ($P<0.05$). The Beclin1 and LC3II/LC3I protein levels indicated enhanced ($P<0.05$ or $P<0.01$), with lower P62 levels in IR rats with ISO treatment at 20 and 40 mg/kg ($P<0.05$ or $P<0.01$). Moreover, in IR group, LC3II/LC3I level of infarcted areas of rat myocardial tissues exhibited lower than that of non-infarcted myocardial tissues ($P<0.01$). Following ISO intervention, there was reduced LC3II/LC3I protein level ($P<0.01$), whereas higher P62 expression in infarcted areas of IR rat myocardial tissues than in non-infarcted myocardial tissues ($P<0.05$ or $P<0.01$).

Effects of ISO treatment on p-AMPK/AMPK, mTOR/p-mTOR, and p-ULK1(S757)/ULK1 protein expression in IR rat myocardial tissues were investigated using western blot approach (Fig. 2C-D). In rat myocardial tissue non-infarcted areas as presented in Fig. 2C, we observed that IR rats caused lower p-AMPK/AMPK and p-mTOR/mTOR expression whereas elevated p-ULK1(S757)/ULK1 protein expression than control rats ($P<0.05$ or $P<0.01$). The p-mTOR/mTOR and p-ULK1(S757)/ULK1 protein expressions in IR + ISO-10 group exhibited a decrease than in IR group ($P<0.01$). The ISO intervention at

(See figure on next page.)

Fig. 1 ISO treatment attenuated myocardial injury in IR rats. **A** Flowchart of our experiments in rats was constructed; **B** The LVESD, LVEDD, EF, FS, LVSP, and LVEDP values of rats were recorded by echocardiography, $n=6$; **C** The histopathologic diagnosis in rat myocardial tissues were examined by HE staining (magnification 200×, scale bar: 100 μm; magnification 400×, scale bar: 50 μm), $n=3$; **D** Observation of fibrosis in rat heart tissues was made by Masson staining (magnification 100×, scale bar: 200 μm; magnification 200×, scale bar: 100 μm), $n=3$; **E** The TTC staining was utilized to determine the infarcted area of rat heart tissues, $n=6$; F–H: The CK-MB, cTnI, and cTnT levels in rat myocardial tissues were assessed by ELISA assay, $n=6$; I-K: The detection of MDA, SOD, and GSH levels in rat cardiac tissues was carried out, $n=6$; ▲$P<0.05$ and ▲▲$P<0.01$ vs. Con group, ★$P<0.05$ and ★★$P<0.01$ vs. IR group. Note: Con: Control; IR: Ischemia reperfusion; ISO: Isoliquiritigenin; LVESD: Left ventricular end-systolic diameter; LVEDD: Left ventricular end-diastolic diameter; EF: Ejection fraction; FS: Fractional shortening; LVSP: Left ventricular peak systolic pressure; LVEDP: Left ventricular end diastolic pressure; ELISA: Enzyme linked immunosorbent assay; CK-MB: Creatine kinase-MB; cTn-I: Cardiac troponin-I; cTn-T: Cardiac troponin-T; HE: Hematoxylin–eosin; TTC: 2,3,5-triphenyltetrazolium chloride; MDA: Malondialdehyde; SOD: Superoxide dismutase; GSH: Glutathione

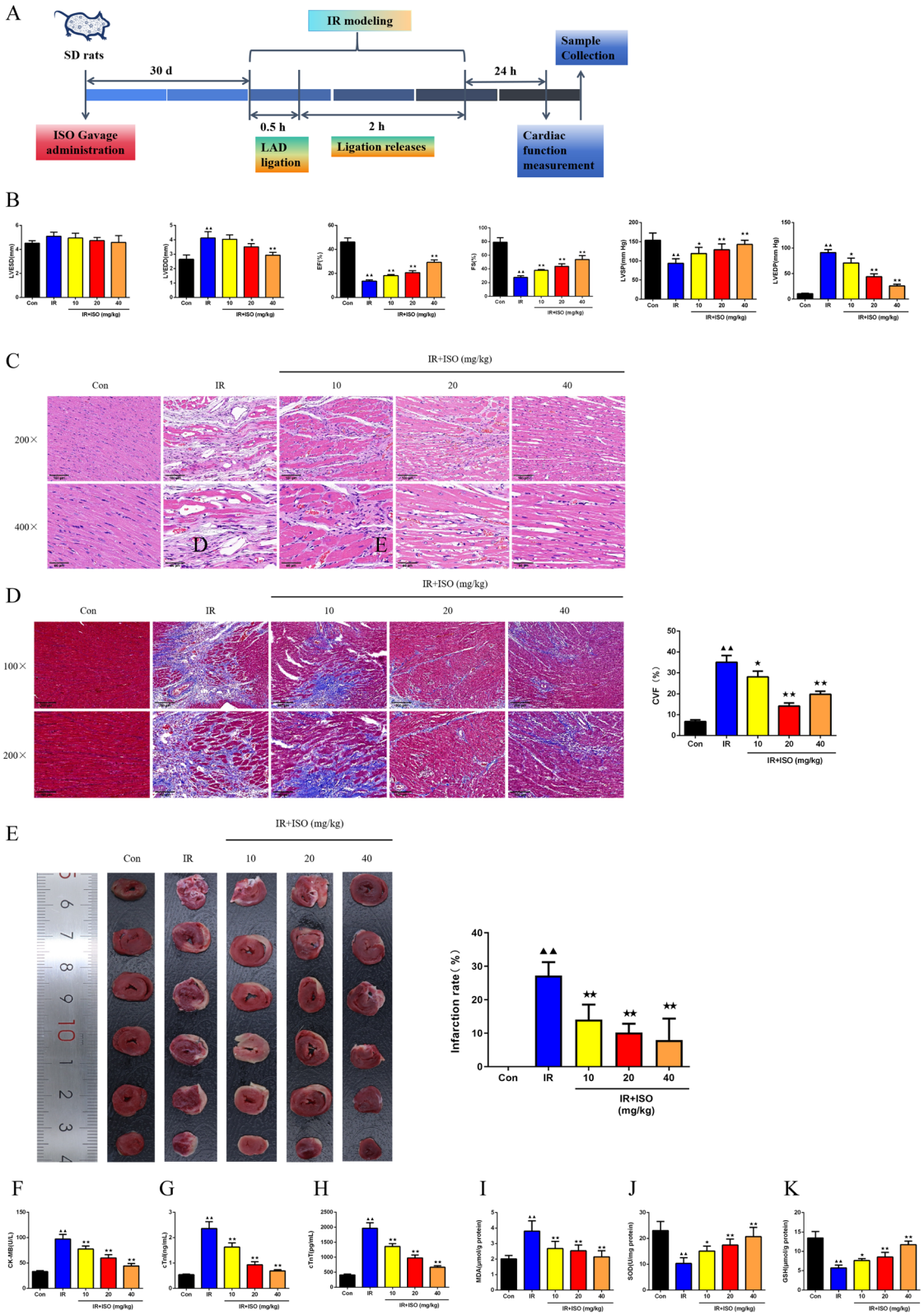

Fig. 1 (See legend on previous page.)

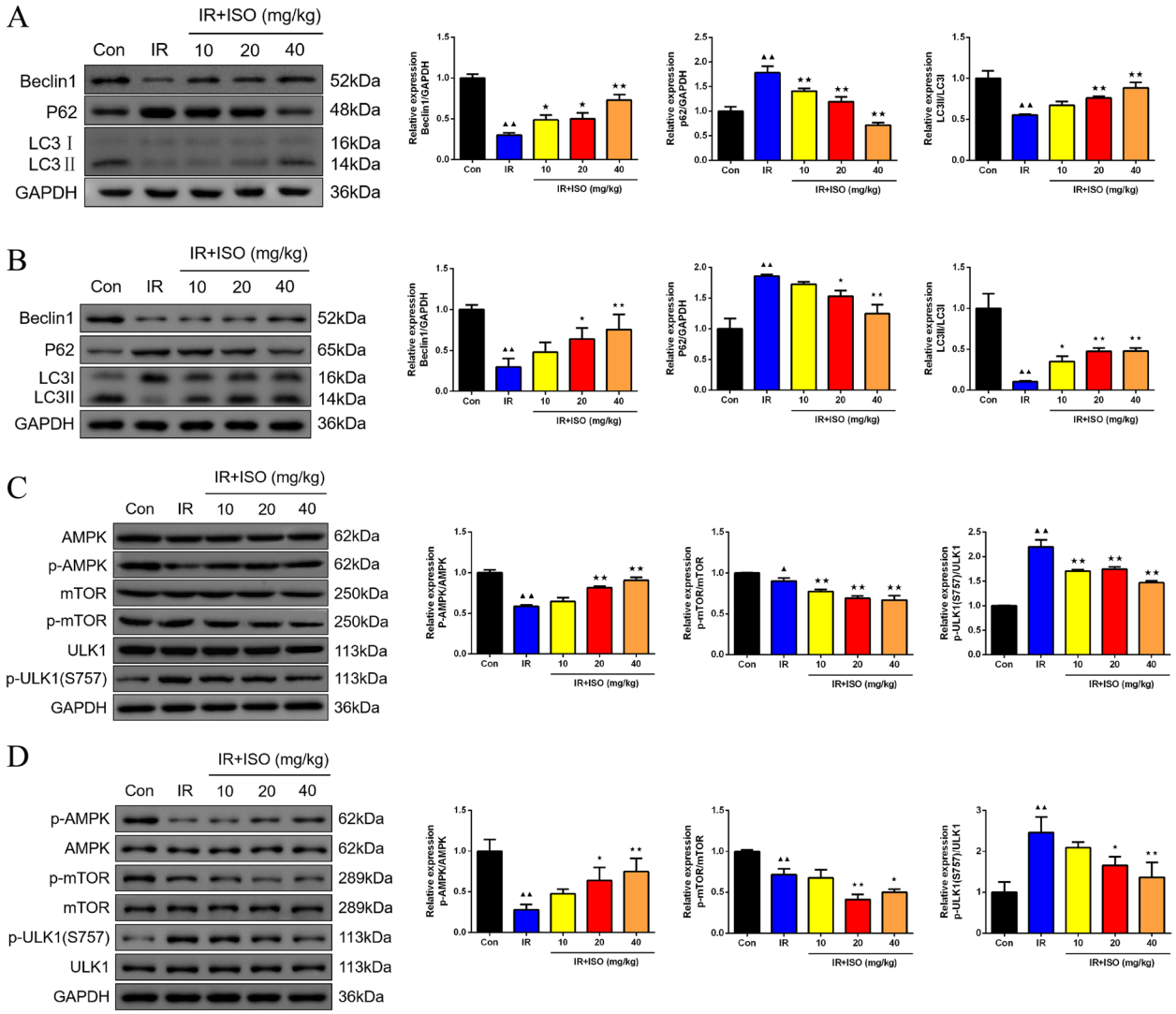

Fig. 2 ISO treatment induced autophagy by AMPK/mTOR/ULK1 pathway in IR rats. The measurement of Beclin1, P62, and LC3II/LC3I protein expression in non-infarcted (A) and infarcted areas (B) of rat myocardial tissues was constructed by western blot assay, $n=3$; The western blot assay was employed to detect p-AMPK/AMPK, mTOR/p-mTOR, and p-ULK1(S757)/ULK1 protein expression in IR rat myocardial tissues in non-infarcted (C) and infarcted areas (D), $n=3$; ▲$P<0.05$ and ▲▲$P<0.01$ vs. Con group, ★$P<0.05$ and ★★$P<0.01$ vs. IR group. **Note**: Con: Control; IR: Ischemia reperfusion; ISO: Isoliquiritigenin

20 and 40 mg/kg for IR rats led to enhanced p-AMPK/AMPK levels, whereas diminished p-mTOR/mTOR and p-ULK1(S757)/ULK1 expression than rats in IR group ($P<0.01$). Moreover, there were decreased p-AMPK/AMPK and p-mTOR/mTOR protein expression (Fig. 2D, $P<0.01$), whereas increased p-ULK1(S757)/ULK1 protein levels in infarction areas of IR rat myocardial tissues than in control rats ($P<0.01$). Following 20 and 40 mg/kg of ISO intervention, p-AMPK/AMPK protein presented an increase in IR rats ($P<0.05$ or $P<0.01$), with an reduction of p-mTOR/mTOR and p-ULK1(S757)/ULK1 expression ($P<0.05$ or $P<0.01$).

ISO treatment promoted cell viability and inhibited apoptosis in IR H9c2 cells

In Fig. 2A-B, CCK8 assay was conducted to measure cell viability of H9c2 cells exposed to various dosages (0.1, 1, 10, 100, 1000 μmol/L) of ISO and following IR modeling. The findings indicated that different dosages of ISO treatment (0.1, 1, 10, 100, 1000 μmol/L) led to no impact on normal H9c2 cell viability (Fig. 3A). After IR modeling, 1, 10, and 100 μmol/L of ISO treatment led to a dose-dependent gradual increase in cell viability (Fig. 3B, $P<0.01$). However, a decrease in cell viability occurred under 1000 μmol/L ISO treatment, which exhibited

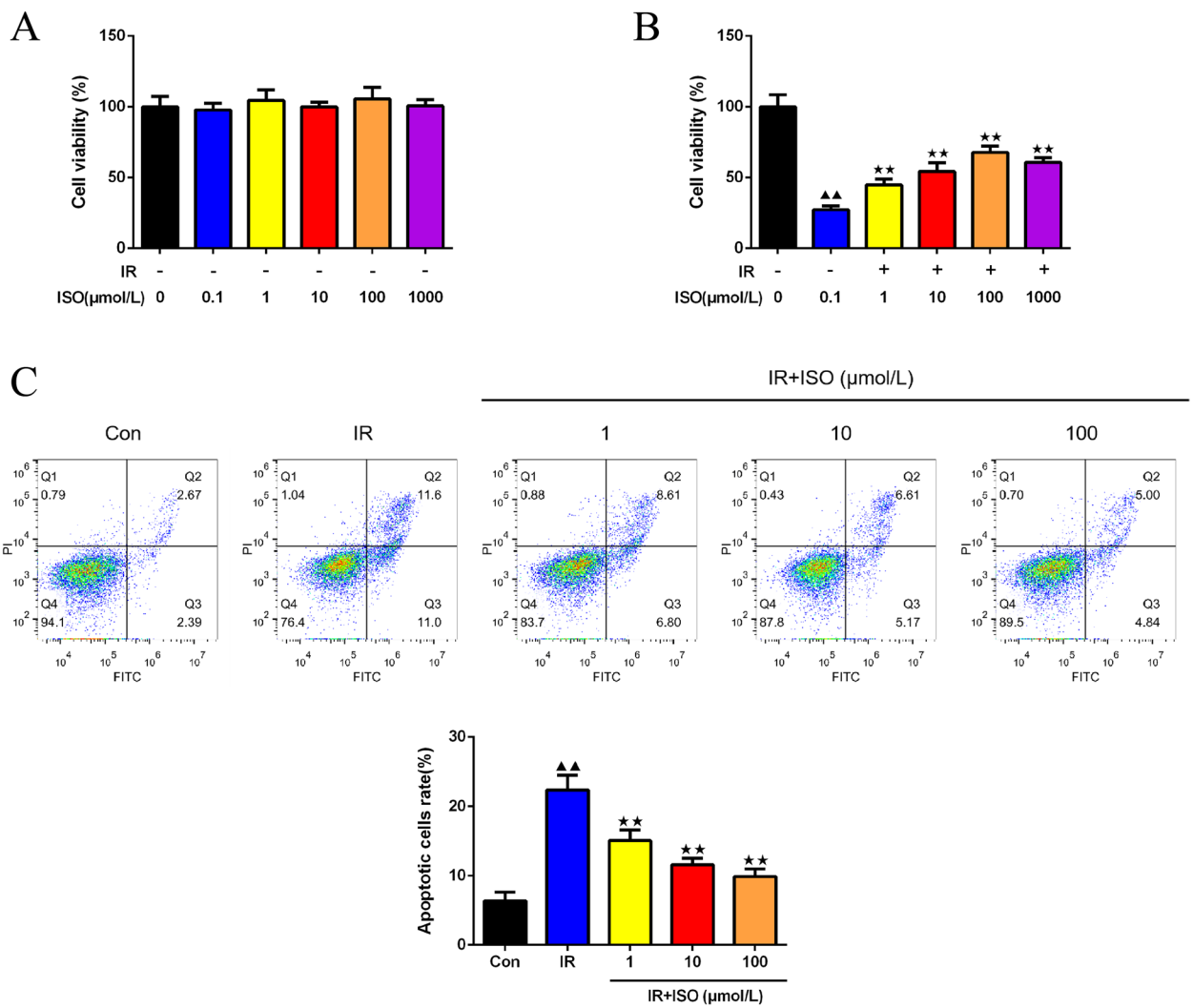

Fig. 3 ISO treatment promoted cell viability and inhibited apoptosis in IR H9c2 cells. Assessment of H9c2 cell viability under various dosages (0.1, 1, 10, 100, 1000 μmol/L) of ISO treatment (A) and following IR modeling (B) was performed by CCK8 assay, $n=6$; C: The apoptotic cell rates of H9c2 cells were assessed using FC, $n=3$; ▲$P<0.05$ and ▲▲$P<0.01$ vs. Con group, ★$P<0.05$ and ★★$P<0.01$ vs. IR group. Note: Con: Control; IR: Ischemia reperfusion; ISO: Isoliquiritigenin; FC: flow cytometry

cytotoxicity. Subsequently, examination on apoptosis of H9c2 cells by FC assay demonstrated a highly significant increase of H9c2 cells with IR modeling (Fig. 3C, $P<0.01$). The apoptosis rate of 1, 10, and 100 μmol/L ISO treatment group decreased than IR H9c2 cells ($P<0.01$).

ISO treatment caused autophagy induction by AMPK/mTOR/ULK1 pathway in IR H9c2 cells

In Fig. 4A, observation of autophagosome in H9c2 cells was performed by TEM method. The H9c2 cells in IR group presented smaller number of autophagosome than in Control group. Following ISO treatment interventions at 1, 10, and 100 μmol/L, there was a noticeable increase in autophagosome number of H9c2 cells with IR damage. The immunofluorescence assay was employed to detect LC3 expression in H9c2 cells (Fig. 4B). There was decreased LC3 fluorescent expression occurred in IR H9c2 cells ($P<0.01$). Further ISO interventions enhanced LC3 fluorescence intensity ($P<0.05$ or $P<0.01$). The effects of ISO treatment on Beclin1, P62 and LC3 protein expression in H9c2 cells were investigated by western blot approach (Fig. 4C). The IR H9c2 cells exhibited lower Beclin1 and LC3II/LC3I protein levels, whereas enhanced P62 protein than control cells ($P<0.05$ or $P<0.01$). The ISO treatment at 1 μmol/L induced higher Beclin1 protein expression and lower P62 protein expression ($P<0.05$ or $P<0.01$). Moreover, ISO treatment at 10 and 100 μmol/L for IR H9c2 cells led to increased Beclin1

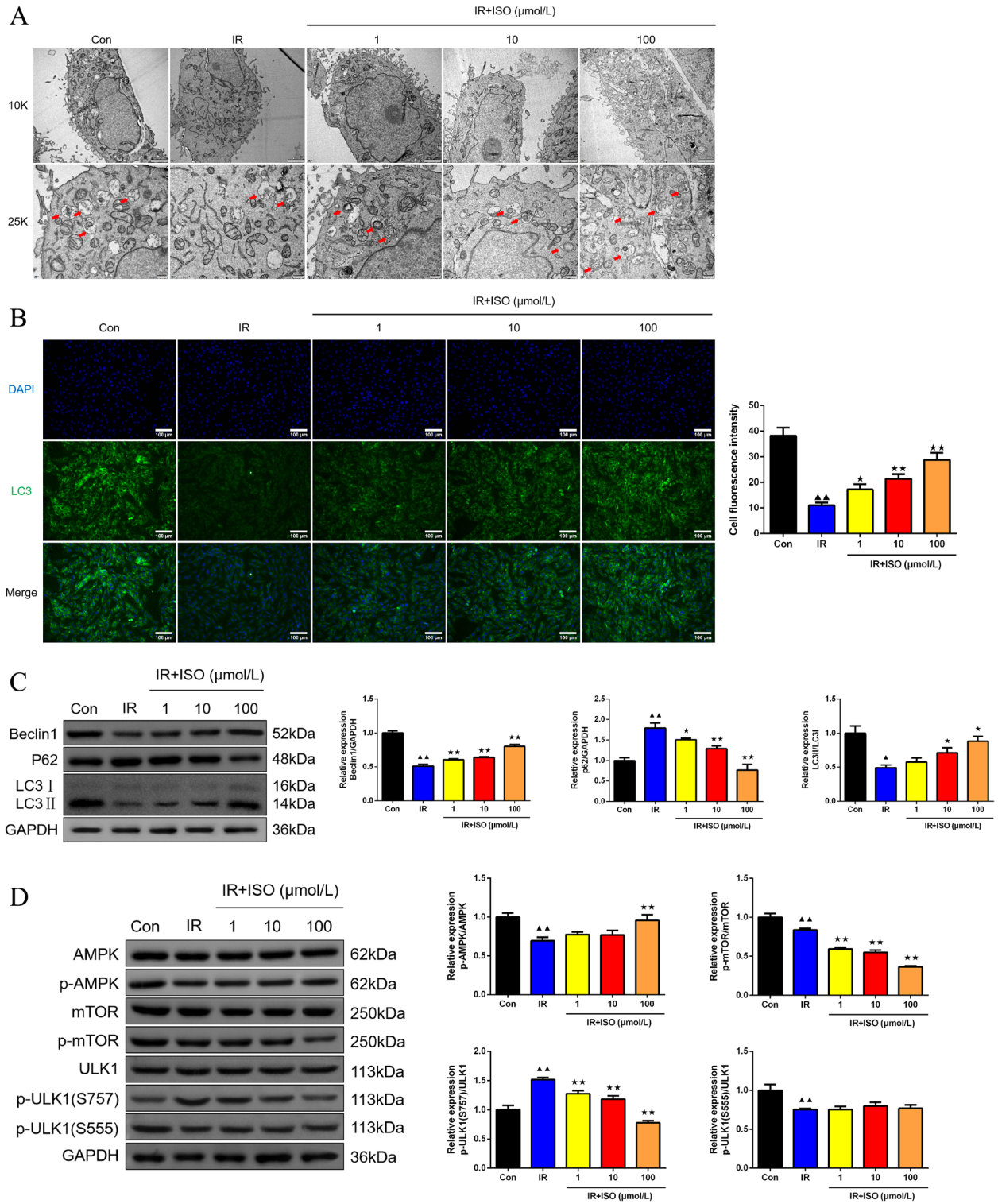

Fig. 4 ISO treatment caused autophagy induction by AMPK/mTOR/ULK1 pathway in IR H9c2 cells. **A** The detection of H9c2 cell ultra-structure was completed by TEM (magnification 10.0 k×, scale bar: 2 μm; magnification 25.0 k×, scale bar: 500 nm), red arrows showed autophagosome, $n=6$; **B** The immunofluorescence assay was conducted to measure LC3 fluorescence expression in H9c2 cells (magnification 200×, scale bar: 100 μm), $n=6$; **C** Western blot was employed to measure Beclin1, P62 and LC3II/LC3I protein expression in H9c2 cells, $n=3$; **D** The p-AMPK/AMPK, p-mTOR/mTOR, and p-ULK1(S757)/ULK1, and p-ULK1(S555)/ULK1 protein expression of H9c2 cells was tested by western blot assay, $n=3$; ▲$P<0.05$ and ▲▲$P<0.01$ vs. Con group, ★$P<0.05$ and ★★$P<0.01$ vs. IR group. Note: Con: Control; IR: Ischemia reperfusion; ISO: Isoliquiritigenin; TEM: Transmission electron microscopy

protein expression as well as LC3II/LC3I levels, whereas lowered P62 protein expression ($P<0.05$ or $P<0.01$). Western blot was utilized for measurement of p-AMPK/AMPK, mTOR/p-mTOR, and p-ULK1(S757)/ULK1 protein expression in H9c2 cells (Fig. 4D). The IR H9c2 cells demonstrated lower p-AMPK/AMPK, p-mTOR/mTOR and p-ULK1(S555)/ULK1 protein, with higher p-ULK1(S757)/ULK1 protein expression than in control cells ($P<0.01$). The IR + ISO-1 and IR + ISO-10 groups exhibited reduced p-mTOR/mTOR and p-ULK1(S757)/ULK1 protein expression than in IR groups ($P<0.01$). Furthermore, in IR + ISO-100 group, it presented lower p-mTOR/mTOR and p-ULK1(S757)/ULK protein expression, whereas increased p-AMPK/AMPK expression than in IR H9c2 cells ($P<0.01$).

Discussion

The current most clinically effective intervention for myocardial ischemia is prompt reperfusion, which improves myocardial function to a certain extent, although it is likewise accompanied by excessive reactive oxygen species production, enhanced apoptosis, and autophagy dysfunction, thereby diminishing therapeutic efficacy and inducing irreversible myocardial damage and larger infarct area [22]. As a natural extraction, ISO has been confirmed that it owns diverse biological functions in different areas of disease investigations [23]. The anti-tumor activity of ISO treatment can be exerted by regulating autophagy levels, and it has been found to inhibition of pancreatic cancer progression by blocking p38 MAPK-regulated autophagy [12, 24]. In myocardial infarction mice, ISO treatment performed protection on myocardial tissues through inhibition of inflammatory responses as well as activation of JAK2/STAT3 signaling pathway to alleviate myocardial IR injury in rats [9, 10]. Therefore, in our study, we explored therapeutic effects and mechanisms of ISO treatment on myocardial IR in depth based on establishment of IR rat models and H9c2 cell models. Representative and specific markers in serum for determination of myocardial injury include CK-MB, cTnI, and cTnT, as well as major criterion for assessment of myocardial infarction area [25]. Myocardial tissues of IR-induced rats were under stress, with significantly elevated levels of CK-MB, cTnI, and cTnT, and subsequent treatment lowered these myocardial injury marker levels and enhanced myocardial function [26, 27], which was consistent with our findings.

Autophagy, as an essential pathway involved in cell survival, is critical for myocardial function [28]. Increasing number of studies have revealed that autophagy is extensively participated in IR development, so that modulation of autophagy has also become a potential strategy to attenuate IR injury with more attention from researchers. Both in vivo and in vitro studies have evidenced that increasing autophagy level is able to mitigate cardiomyocyte damage [13, 15]. Chen et al. observed that ISO treatment induced autophagy as well as reduced apoptosis, thereby inhibiting development of cancer cells [11]. What's more, under effective anti-tumor dosages, ISO exhibited minimal cytotoxic effects on normal tissues in vitro and in vivo [11]. The CCK8 results of our study also showed a non-significant effect on cell viability after ISO intervention. FC test findings indicated that ISO intervention lowered apoptosis rate of IR modeling H9c2 cells. Zhang et al. observed that a four-compound, including ISO, were capable of exerting myocardial protection in IR mice and H9c2 cells, possessing an inhibition of TNF-α/NF-κB pathway, and thereby may be a potential therapeutic treatment for myocardial infarction [29]. On this basis, in addition to exploration of autophagy status in rat myocardial tissues, we also conducted studies on effects of ISO intervention on autophagy in H9c2 cells. Beclin1 and P62, as a critical gene and an important autophagy-related mediator, respectively, reflect autophagic activity and degradation ability [30, 31]. LC3 acts as an autophagy signature protein, and LC3I isoform is sheared into LC3II isoform after autophagy occurs, as a result, LC3II/LC3I ratio can be employed to detect degree of autophagy [30]. As gold standard to detect autophagosome, TEM was also performed in our study. Concordant with findings of Lei et al. [12], our data demonstrated a significant attenuation of Beclin1 expression and LC3II/LC3I levels whereas an increase in P62 protein expression in IR rat myocardial tissues and IR-modeled H9c2 cells. After ISO intervention, Beclin1 expression and LC3II/LC3I levels were elevated and P62 expression was diminished with a dose-dependent pattern. These outcomes supported the ability of ISO to activate autophagic process and thus protect myocardial function. Moreover, myocardial infarction led to impaired autophagy, consistent with our preliminary findings [32], although only with lower LC3II/LC3I level of infarcted areas than in non-infarcted IR myocardial tissues.

AMPK, as an upstream molecule of mTOR, is a classical autophagy pathway protein that regulates energy metabolism and autophagy [33]. Activation of AMPK contributes to decreased mTOR activity and increased autophagy in myocardial ischemia/hypoxia injury [34]. AMPK and mTOR perform autophagy regulation through modulation of ULK1 phosphorylation [16]. Research evidence suggests that AMPK/mTOR/ULK1 signaling represents an essential pathway for autophagy regulation [35]. Several studies have revealed that AMPK/mTOR/ULK1 signaling also mediates IR injury therapy [18, 36]. In addition, ISO intervention was demonstrated

to be capable of an improvement in contractile dysfunction in hypoxic cardiomyocytes through AMPK signaling pathway [17]. Consequently, we further explored mechanism by which ISO regulated autophagy levels with detection of AMPK/mTOR/ULK1-related proteins in rat myocardial tissues and H9c2 cells. In both IR rat myocardial tissues and IR modeling H9c2 cells, there were inhibited p-AMPK/AMPK and p-mTOR/mTOR levels whereas an increase in p-ULK1(Ser757)/ULK1 levels. AMPK activation at ULK1 is mainly performed by two following mechanisms: direct activation of AMPK with ULK1-Ser555 phosphorylation and indirect activation of AMPK through inhibiting ULK1-Ser757 phosphorylation via mTOR [37]. A main component of Ginseng attenuated myocardial fibrosis, mainly by activating autophagy with AMPK activation, in turn inhibiting phosphorylation of mTOR and ULK1-Ser757, in accordance with findings of the present study [18]. Our findings revealed that after ISO intervention, AMPK activation and inhibition of mTOR and ULK1-Ser757 phosphorylation were done, whereas no significant changes of ULK1-Ser555 phosphorylation. From these above outcomes, we hypothesized that ISO intervention may not directly activate AMPK by phosphorylating ULK1-Ser555, but may indirectly perform AMPK activation through inhibiting ULK1-Ser757 phosphorylation via mTOR, thereby activating development of autophagy process and protecting myocardium from IR injury.

In conclusion, our subject provided an in-depth exploration of mechanism of whether ISO can ameliorate myocardial IR injury. ISO intervention caused enhancement of myocardial function, decrease of CK-MB, cTnI, cTnT expression, and inhibition of cardiomyocyte apoptosis. Furthermore, ISO treatment may achieve attenuation of myocardial IR injuries through AMPK/mTOR/ULK1 signaling-mediated activation of autophagy. Both in vitro and in vivo findings suggested that ISO treatment may has potential as a candidate for myocardial IR injury therapy. As a preliminary study, our results still need to be combined with clinical study data to complete further corroboration.

Abbreviations

IR	Ischemia reperfusion
ISO	Isoliquiritigenin
LAD	Left anterior descending
LVESD	Left ventricular end-systolic diameter
LVEDD	Left ventricular end-diastolic diameter
EF	Ejection fraction
FS	Fractional shortening
LVSP	Left ventricular peak systolic pressure
LVEDP	Left ventricular end diastolic pressure
MAD	Malondialdehyde
SOD	Superoxide dismutase
GSH	Glutathione
Con	Control
CCK-8	Cell counting kit-8
FC	Flow cytometry
TEM	Transmission electron microscopy

Supplementary Information

The online version contains supplementary material available at https://doi.org/10.1186/s12872-024-04054-z.

Supplementary Material 1.

Supplementary Material 2.

Acknowledgements
Not applicable.

Authors' contributions
Conception and design of the research: Li Zhang, Zhenfeng Chen
Acquisition of data: Yingwei Zhu
Analysis and interpretation of data: Liying Shen, Yingwei Zhu, Feng Shen
Statistical analysis: Liying Shen, Weiwei Yu
Drafting the manuscript: Liying Shen
Revision of manuscript for important intellectual content: Liying Shen and Li Zhang
Final approval of the version to be published: All authors
Agreement to be accountable for all aspects of the work ensuring that questions related to the accuracy or integrity of the work are appropriately investigated and resolved: Liying Shen, Yingwei Zhu, Zhenfeng Chen, Feng Shen, Weiwei Yu, Li Zhang.

Funding
This study was supported by Huzhou Cardiovascular and Cerebrovascular Disease Discipline Group [grant no. XKQ-HT-202102A] and Public Technology Applied Research Program of Huzhou City [grant no. 2023GY10].

Availability of data and materials
The datasets generated during and/or analyzed during the current study are available from the corresponding author upon reasonable request.

Declarations

Ethics approval and consent to participate
The Animal Experimentation Ethics Committee of Zhejiang Eyong Pharmaceutical Research and Development Centre approved the ethical conduct of animal experiments (SYXK(Zhe) 2023–0027). All methods reported in our study were in accordance with ARRIVE guidelines (https://arriveguidelines.org) for the reporting of animal experiments.

Consent for publication
Not applicable.

Competing interests
The authors declare no competing interests.

Received: 29 February 2024 Accepted: 16 July 2024
Published online: 09 August 2024

References

1. Tsao CW, Aday AW, Almarzooq ZI, Anderson CAM, Arora P, Avery CL, Baker-Smith CM, Beaton AZ, Boehme AK, Buxton AE, Commodore-Mensah Y, Elkind MSV, Evenson KR, Eze-Nliam C, Fugar S, Generoso G, Heard DG, Hiremath S, Ho JE, Kalani R, Kazi DS, Ko D, Levine DA, Liu J, Ma J, Magnani JW, Michos ED, Mussolino ME, Navaneethan SD, Parikh NI, Poudel R, Rezk-Hanna M, Roth GA, Shah NS, St-Onge MP, Thacker EL, Virani SS, Voeks JH, Wang NY, Wong ND, Wong SS, Yaffe K, Martin SS. Heart

Disease and Stroke Statistics-2023 Update: A Report From the American Heart Association. Circulation. 2023;147:e93–621.
2. Wen C, Lan M, Tan X, Wang X, Zheng Z, Lv M, Zhao X, Luo H, Liu Y, Wei P, Yue R, Hu H, Guo L. GSK3β Exacerbates Myocardial Ischemia/Reperfusion Injury by Inhibiting Myc. Oxid Med Cell Longev. 2022;2022:2588891.
3. Ding X, Zhu C, Wang W, Li M, Ma C, Gao B. SIRT1 is a regulator of autophagy: implications for the progression and treatment of myocardial ischemia-reperfusion. Pharmacol Res. 2023;199:106957.
4. Heusch G. Myocardial ischaemia-reperfusion injury and cardioprotection in perspective, Nature reviews. Cardiology. 2020;17:773–89.
5. Liu Y, Xu J, Wu M, Kang L, Xu B. The effector cells and cellular mediators of immune system involved in cardiac inflammation and fibrosis after myocardial infarction. J Cell Physiol. 2020;235:8996–9004.
6. Gu X, Shi Y, Chen X, Sun Z, Luo W, Hu X, Jin G, You S, Qian Y, Wu W, Liang G, Wu G, Chen Z, Chen X. Isoliquiritigenin attenuates diabetic cardiomyopathy via inhibition of hyperglycemia-induced inflammatory response and oxidative stress. Phytomedicine. 2020;78:153319.
7. Huang X, Shi Y, Chen H, Le R, Gong X, Xu K, Zhu Q, Shen F, Chen Z, Gu X, Chen X, Chen X. Isoliquiritigenin prevents hyperglycemia-induced renal injuries by inhibiting inflammation and oxidative stress via SIRT1-dependent mechanism. Cell Death Dis. 2020;11:1040.
8. Zhan C, Yang J. Protective effects of isoliquiritigenin in transient middle cerebral artery occlusion-induced focal cerebral ischemia in rats. Pharmacol Res. 2006;53:303–9.
9. An W, Yang J, Ao Y. Metallothionein mediates cardioprotection of isoliquiritigenin against ischemia-reperfusion through JAK2/STAT3 activation. Acta Pharmacol Sin. 2006;27:1431–7.
10. Yao D, Shi B, Wang S, Bao L, Tan M, Shen H, Zhang Z, Pan X, Yang Y, Wu Y, Gong K. Isoliquiritigenin Ameliorates Ischemia-Induced Myocardial Injury via Modulating the Nrf2/HO-1 Pathway in Mice. Drug Des Dev Ther. 2022;16:1273–87.
11. Chen HY, Huang TC, Shieh TM, Wu CH, Lin LC, Hsia SM. Isoliquiritigenin Induces Autophagy and Inhibits Ovarian Cancer Cell Growth. Int J Mol Sci. 2017;18:2025.
12. Song L, Luo Y, Li S, Hong M, Wang Q, Chi X, Yang C. ISL Induces Apoptosis and Autophagy in Hepatocellular Carcinoma via Downregulation of PI3K/AKT/mTOR Pathway in vivo and in vitro. Drug Des Dev Ther. 2020;14:4363–76.
13. Xing Y, Sui Z, Liu Y, Wang MM, Wei X, Lu Q, Wang X, Liu N, Lu C, Chen R, Wu M, Wang Y, Zhao YH, Guo F, Cao JL, Qi J, Wang W. Blunting TRPML1 channels protects myocardial ischemia/reperfusion injury by restoring impaired cardiomyocyte autophagy. Basic Res Cardiol. 2022;117:20.
14. Loos B, Genade S, Ellis B, Lochner A, Engelbrecht AM. At the core of survival: autophagy delays the onset of both apoptotic and necrotic cell death in a model of ischemic cell injury. Exp Cell Res. 2011;317:1437–53.
15. Yu YW, Liu S, Zhou YY, Huang KY, Wu BS, Lin ZH, Zhu CX, Xue YJ, Ji KT. Shexiang Baoxin Pill attenuates myocardial ischemia/reperfusion injury by activating autophagy via modulating the ceRNA-Map3k8 pathway. Phytomedicine. 2022;104:154336.
16. Wang JF, Mei ZG, Fu Y, Yang SB, Zhang SZ, Huang WF, Xiong L, Zhou HJ, Tao W, Feng ZT. Puerarin protects rat brain against ischemia/reperfusion injury by suppressing autophagy via the AMPK-mTOR-ULK1 signaling pathway. Neural Regen Res. 2018;13:989–98.
17. Zhang X, Zhu P, Zhang X, Ma Y, Li W, Chen JM, Guo HM, Bucala R, Zhuang J, Li J. Natural antioxidant-isoliquiritigenin ameliorates contractile dysfunction of hypoxic cardiomyocytes via AMPK signaling pathway. Mediators Inflamm. 2013;2013:390890.
18. Wang L, Yuan D, Zheng J, Wu X, Wang J, Liu X, He Y, Zhang C, Liu C, Wang T, Zhou Z. Chikusetsu saponin IVa attenuates isoprenaline-induced myocardial fibrosis in mice through activation autophagy mediated by AMPK/mTOR/ULK1 signaling. Phytomedicine. 2019;58:152764.
19. Zeng J, Chen Y, Ding R, Feng L, Fu Z, Yang S, Deng X, Xie Z, Zheng S. Isoliquiritigenin alleviates early brain injury after experimental intracerebral hemorrhage via suppressing ROS- and/or NF-κB-mediated NLRP3 inflammasome activation by promoting Nrf2 antioxidant pathway. J Neuroinflammation. 2017;14:119.
20. Yang Y, Shao M, Yao J, Yang S, Cheng W, Ma L, Li W, Cao J, Zhang Y, Hu Y, Li C, Wang Y, Wang W. Neocryptotanshinone protects against myocardial ischemia-reperfusion injury by promoting autolysosome degradation of protein aggregates via the ERK1/2-Nrf2-LAMP2 pathway. Phytomedicine. 2023;110:154625.
21. Lv D, Luo M, Cheng Z, Wang R, Yang X, Guo Y, Huang L, Li X, Huang B, Shen J, Luo S, Yan J. Tubeimoside I Ameliorates Myocardial Ischemia-Reperfusion Injury through SIRT3-Dependent Regulation of Oxidative Stress and Apoptosis. Oxid Med Cell Longev. 2021;2021:5577019.
22. Yang N, Wu L, Zhao Y, Zou N, Liu C. MicroRNA-320 involves in the cardioprotective effect of insulin against myocardial ischemia by targeting survivin. Cell Biochem Funct. 2018;36:166–71.
23. Liu JQ, Zhao XT, Qin FY, Zhou JW, Ding F, Zhou G, Zhang XS, Zhang ZH, Li ZB. Isoliquiritigenin mitigates oxidative damage after subarachnoid hemorrhage in vivo and in vitro by regulating Nrf2-dependent Signaling Pathway via Targeting of SIRT1. Phytomedicine. 2022;105:154262.
24. Zhang Z, Chen WQ, Zhang SQ, Bai JX, Liu B, Yung KK, Ko JK. Isoliquiritigenin inhibits pancreatic cancer progression through blockade of p38 MAPK-regulated autophagy. Phytomedicine. 2022;106:154406.
25. Xiao Y, Chen W, Zhong Z, Ding L, Bai H, Chen H, Zhang H, Gu Y, Lu S. Electroacupuncture preconditioning attenuates myocardial ischemia-reperfusion injury by inhibiting mitophagy mediated by the mTORC1-ULK1-FUNDC1 pathway. Biomed Pharmacother. 2020;127:110148.
26. Fan Z, Cai L, Wang S, Wang J, Chen B. Baicalin Prevents Myocardial Ischemia/Reperfusion Injury Through Inhibiting ACSL4 Mediated Ferroptosis. Front Pharmacol. 2021;12:628988.
27. Hu S, Jiang L, Yan Q, Zhou C, Guo X, Chen T, Ma S, Luo Y, Hu C, Yang F, Yuan L, Ma X, Zeng J. Evidence construction of baicalin for treating myocardial ischemia diseases: A preclinical meta-analysis. Phytomedicine. 2022;107:154476.
28. Li Y, Liang P, Jiang B, Tang Y, Liu X, Liu M, Sun H, Chen C, Hao H, Liu Z, Xiao X. CARD9 promotes autophagy in cardiomyocytes in myocardial ischemia/reperfusion injury via interacting with Rubicon directly. Basic Res Cardiol. 2020;115:29.
29. Zhang X, Chen Q, Zhao J, Zhao W, Fan N, Wang Y, Chen H, Rong J. A four-compound remedy AGILe protected H9c2 cardiomyocytes against oxygen glucose deprivation via targeting the TNF-α/NF-κB pathway: Implications for the therapy of myocardial infarction. Front Pharmacol. 2023;14:1050970.
30. Zhang H, Ye J, Wang X, Liu Z, Chen T, Gao J. Therapeutic Effect and Mechanism of Cinnamyl Alcohol on Myocardial Ischemia-Reperfusion Injury. Evid Based Complement Alternat Med. 2022;2022:5107948.
31. Hu L, Xie H, Liu X, Potjewyd F, James LI, Wilkerson EM, Herring LE, Xie L, Chen X, Cabrera JC, Hong K, Liao C, Tan X, Baldwin AS, Gong K, Zhang Q. TBK1 Is a Synthetic Lethal Target in Cancer with VHL Loss. Cancer Discov. 2020;10:460–75.
32. Marzoog BA. Autophagy Behavior in Post-myocardial Infarction Injury. Cardiovasc Hematol Disord: Drug Targets. 2023;23:2–10.
33. Lin M, Hua R, Ma J, Zhou Y, Li P, Xu X, Yu Z, Quan S. Bisphenol A promotes autophagy in ovarian granulosa cells by inducing AMPK/mTOR/ULK1 signalling pathway. Environ Int. 2021;147:106298.
34. Sciarretta S, Hariharan N, Monden Y, Zablocki D, Sadoshima J. Is autophagy in response to ischemia and reperfusion protective or detrimental for the heart? Pediatr Cardiol. 2011;32:275–81.
35. Xi X, Zou C, Ye Z, Huang Y, Chen T, Hu H. Pioglitazone protects tubular cells against hypoxia/reoxygenation injury through enhancing autophagy via AMPK-mTOR signaling pathway. Eur J Pharmacol. 2019;863:172695.
36. Chen QS, Shen A, Dai JW, Li TT, Huang WF, Shi K, Deng Y, Pan L, Wei XF, Wu ZJ. IL37 overexpression inhibits autophagy and apoptosis induced by hepatic ischemia reperfusion injury via modulating AMPK/mTOR/ULLK1 signalling pathways. Life Sci. 2021;276:119424.
37. Xiong R, Zhou XG, Tang Y, Wu JM, Sun YS, Teng JF, Pan R, Law BY, Zhao Y, Qiu WQ, Wang XL, Liu S, Wang YL, Yu L, Yu CL, Mei QB, Qin DL, Wu AG. Lychee seed polyphenol protects the blood-brain barrier through inhibiting Aβ(25–35)-induced NLRP3 inflammasome activation via the AMPK/mTOR/ULK1-mediated autophagy in bEnd.3 cells and APP/PS1 mice. Phytother Res. 2021;35:954–73.

Publisher's Note